

## RECENT RESULTS CONCERNING THE MODELLING OF POLYCRYSTALLINE PLASTICITY AT LARGE STRAINS

P. LIPINSKI, A. NADDARI and M. BERVEILLER  
Laboratoire de Physique et Mécanique des Matériaux,  
UA-CNRS-University of Metz-ENIM, France

**Abstract**—The general method which works for the case of linear properties of heterogeneous materials is taken as a pattern for the derivation of the local strain field in time-independent plasticity of polycrystals. The localization procedure leads to an integral equation solved by the self-consistent scheme approximation. Significant results concerning elastoplastic tangent moduli, initial and subsequent yield surfaces, residual stresses and stored energy and texture development for FCC and BCC polycrystals are reported.

### I. INTRODUCTION

During large elastoplastic straining of polycrystals, a deep change of the material internal state is commonly observed. This change of state induces a strongly path-dependent overall behaviour. Classical phenomenological description of such a complex behaviour needs numerous parameters rather difficult to identify.

Since the pioneering work of Taylor (1938), a great effort has been developed in order to incorporate more microstructure, micromechanics and physics into a continuous and discrete description of the polycrystalline inelastic behaviour at finite deformation. By assuming a uniform plastic strain field over the whole sample the Taylor hypothesis cannot take into account isotropic hardening due to the increase of dislocation density and kinematic hardening due to the dislocations associated with internal stresses. In Mura's (1982) terminology this assumption implies that only impotent distributions of dislocations can exist which is certainly not the case.

More recently, the general methods (Kröner, 1967; Dederichs and Zeller, 1973) which work for the case of linear properties of heterogeneous materials were adapted for the derivation of the local strain rate field from the imposed boundary conditions and the deviations of the local incremental moduli from those of a fictitious homogeneous solid (Berveiller and Zaoui, 1984; Lipinski and Berveiller, 1989). This formulation leads to an integral equation relating the local strain rate field to the (uniform) strain rate imposed at the boundary.

In the case of a topology corresponding to the inclusion-matrix situation, this integral equation reduces to the classical Eshelby's (1957) inhomogeneous inclusion problem, and, in the context of microheterogeneous solids, to the self-consistent scheme proposed by Kröner (1958), Hill (1965), and developed among others by Hutchinson (1970), Budiansky and Wu (1962), Berveiller and Zaoui (1979), Iwakuma and Nemat-Nasser (1984) and Lipinski and Berveiller (1989).

The systematic large strain self-consistent approach was developed numerically by Iwakuma and Nemat-Nasser (1984) using a two-dimensional model in uniaxial loading and assuming a given set of two potentially active slip systems. This simplification neglects one of the most important problems in polycrystalline plasticity corresponding to the fact that, for FCC or BCC metals, there are at least twelve glide systems available. One main task of polycrystalline modelling is to detect among all the crystallographically possible systems, those which are potentially active (resolved shear stress equals the critical shear stress) and among this set the subset corresponding to effectively active systems. By neglecting this multislip mechanism, second-order internal stresses and cross-hardening between slip systems are not correctly described in radial as well as in non-radial loading paths. As a

consequence, induced plastic anisotropy related to texture formation is badly described. These simplifications are not made in the Lipinski and Berveillers' (1989) approach, which formulated a truly three-dimensional self-consistent approach and applied it to many problems (Lipinski *et al.*, 1990).

In this contribution, the theory is not reintroduced since it was published elsewhere. Only significant results concerning FCC and BCC metals are presented and discussed. Special attention is given to the evolution of fields describing the internal state and their influence on the overall behaviour. In the last part of the paper we discuss the limitations of such an approach.

## 2. LOCAL BEHAVIOUR AND OVER-ALL RESPONSE

In this section, results concerning the overall behaviour (stress-strain curves, elasto-plastic tangent moduli, initial and subsequent yield surfaces) obtained from the self-consistent formulation are presented. They concern high stacking fault energy FCC metals or BCC metals. First of all, the initial state of the polycrystal has to be defined and the single crystal mechanical response to be identified.

### (a) *Initial state of the polycrystal and single crystal behaviour*

For usual FCC or BCC crystals, the elastic behaviour is almost isotropic and can be defined by the usual Lamé constants  $\lambda$ ,  $\mu$ . Calculation done for anisotropic elasticity does not show a large influence at least for Al or Cu anisotropy. FCC single crystals possess 12 easy slip systems  $\{111\}\langle 110\rangle$  which may glide in two senses, and the same initial critical shear stress  $\tau_0$  for a well-recrystallized material. For BCC crystals, the situation is more complicated. We assume that the pencil glide may be described by two families of slip systems  $\{110\}\langle 111\rangle$ ,  $\{112\}\langle 110\rangle$  having equal or different initial critical shear stresses.

The hardening matrix for both crystal symmetries contains only two terms,  $H_1$  and  $H_2$ , corresponding to weak and strong interactions between the glide systems (see Franciosi, 1983; Franciosi *et al.*, 1980). The weakest term  $H_1$  corresponds to the slope in stage II of a single crystal experiment. It is nearly equal to  $\mu/250$  for FCC crystals and to  $\mu/500$  for BCC crystals. The second term  $H_2$  is deduced from latent hardening experiments and is taken as  $A \times H_1$ ,  $A$  being the anisotropy factor of the hardening matrix. For FCC metals,  $A$  lies between 1 and 3. In our calculations,  $H_1$  and  $A$  are taken as constant during the loading (linear hardening). The initial second-order residual stresses are assumed to be zero for recrystallized materials.

The polycrystalline state of the sample is characterized by the initial shape and orientation of the ellipsoid corresponding to the grains. For a given ellipsoid, the shape is defined by three semi-axis  $a$ ,  $b$  and  $c$  and its orientation with respect to the macroscopic frame by three angles  $(\alpha, \beta, \gamma)$ . In each grain, the orientation of the lattice is described by three Euler angles  $\varphi_1, \phi, \varphi_2$ , corresponding to the choice of Bunge (1969). Finally, for each grain, the volumic fraction is defined by  $f_i$ , and some preliminary numerical tests have shown that, with a sufficient accuracy, the behaviour is well described by 100 grains with initial random orientation.

All these parameters have a physically well-defined meaning and, in principle, they may be obtained from experiments on single or polycrystals. This reduced set of physical parameters is sufficient to reproduce quantitatively many experimentally observed phenomena. In the following, we present results concerning multiaxial stress state for proportional and non-proportional loading paths.

### (b) *Overall behaviour for FCC polycrystals*

Figure 1 presents several results for a tensile test and for various aspect ratios of the initial grain shape (FCC metals). The tensile axis is parallel to the  $c$  axis of grains. For all the curves, one observes the well-established behavior of FCC metals (Jaoul, 1964):

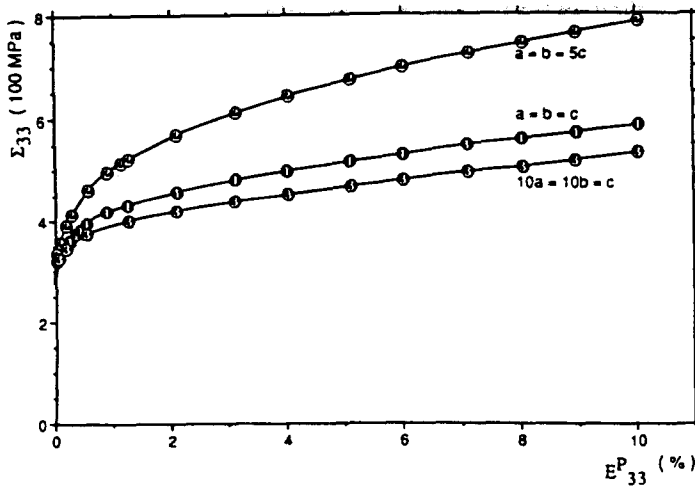


Fig. 1. The influence of the grains shape of tensile curves for a FCC polycrystal.

- a first stage (until 2 or 3% plastic strain) with a parabolic evolution corresponding to the progressive activity of slip systems and whose strongly decreasing hardening is mainly due to internal stresses ;
- a second, almost linear stage (for  $E^p > 3\%$ ) with a slope approximately equal to one hundred times the elastic Young modulus ;
- the difference in the curves for various aspect ratios of the grains is mainly due to the reaction stress between the grains and the matrix.

For a non-monotonic and non-radial loading path, Fig. 2 shows the evolution of the instantaneous elastoplastic tangent moduli during a tensile test in direction 1 until  $E^p$  has reached a value of 0.4% followed by a fully unloading and a subsequent tensile test in direction 2. As expected, a very important and rapid change of the tangent moduli is obtained by an abrupt change in path loading.

In the  $\Sigma_1$ - $\Sigma_2$  stress subspace, the initial yield surface corresponds to the Tresca criterion for plastic offset of 0% and tends to the von Mises ellipse for an offset of 0.2% plastic strain. The yield surfaces are strongly affected by the strain history, i.e. they depend both on the strain amplitude (measured by the von Mises equivalent plastic strain  $\epsilon_{eq}$ ) and prestraining direction. Moreover, the shape of the subsequent yield surfaces is highly dependent on the definition of the plastic offset.

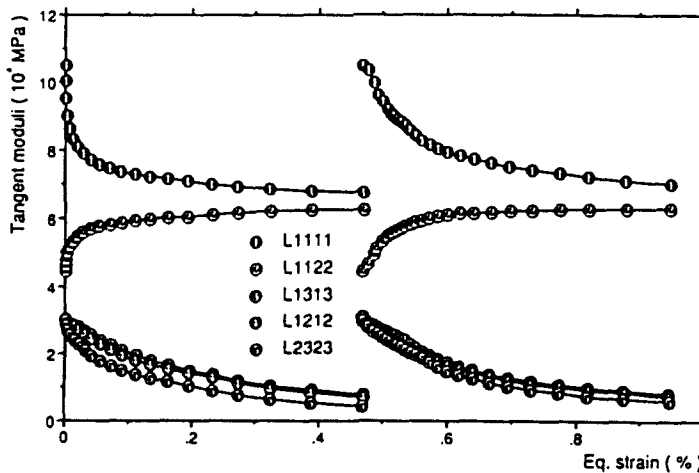


Fig. 2. Tangent moduli evolution during a non-radial loading path.

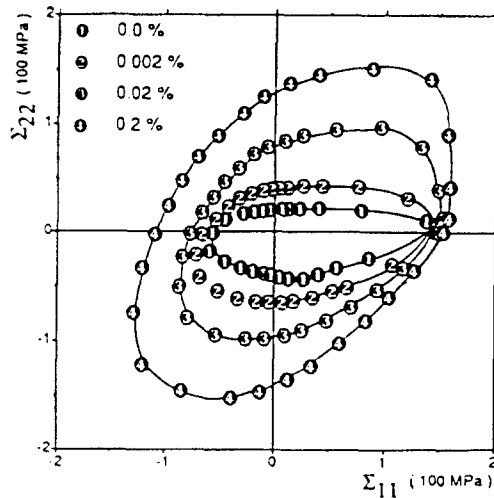


Fig. 3. The subsequent yield surfaces as a function of the definition of the plastic offset.

Figure 3 shows the effect of a small plastic prestrain (tensile test up to 0.4% plastic strain) on the shape of the subsequent yield surface. This shape depends in an important manner on the chosen plastic offset which reflects the effects of the internal stress state introduced by the preloading. It is clear that the influence of the crystallographic and morphological texture is negligible.

For a larger amount of prestrain, the influence of textures becomes predominant even if internal stresses are always present. In the case of BCC metals, Fig. 4a and b shows simultaneously the subsequent yield surfaces and the induced crystallographic texture for two different preloading directions. The random initial crystallographic texture disappears and a strongly path-dependent texture is built, reflecting the plastic anisotropy of the material. The shape of the subsequent yield surfaces is less plastic-offset-dependent than previously; this indicates that the internal stress effect is relatively less important. These phenomena are in agreement with the results presented below and concerning the polycrystal internal state evolution.

### 3. EVOLUTION OF THE INTERNAL STATE OF THE POLYCRYSTAL

Classical self-consistent modelling which takes the grain and the lattice inside the grain as a whole can only give information about the grain's shape and orientation of the lattice. The grain's evolution has a weak impact on the overall behaviour of the material compared with the lattice rotation. The latter may serve as a test for modelling since it is experimentally available by modern X-ray techniques.

The relative misorientation of the grains of the polycrystal and the plastic anisotropy of the single crystal generate, during plastic straining of the material, second-order internal stresses, i.e. the stresses at the grain level which are different from grain to grain. These stresses play an important role in the hardening phenomenon. For instance, in spite of the linear hardening of the single crystal the overall tensile stress-strain curve (Fig. 1) exhibits a non-linear aspect due to these stresses.

The self-consistent modelling enables us to calculate the residual stresses inside each grain and to follow their evolution in the function of the plastic strain. Figure 5 depicts the evolution of the three components of residual stress tensor, namely  $\sigma_{11}$ ,  $\sigma_{22}$  and  $\sigma_{33}$ , during a tensile test in direction 3. A very rapid evolution of these stresses can be observed during the first 3% of plastic strain followed by quasi-linear evolution such that the  $\sigma_{33}$  component is practically equal to one-third of the flow stress. Of course these residual stresses are self-equilibrated. On the other hand the internal stresses contribute to the increase of the stored energy of the material.

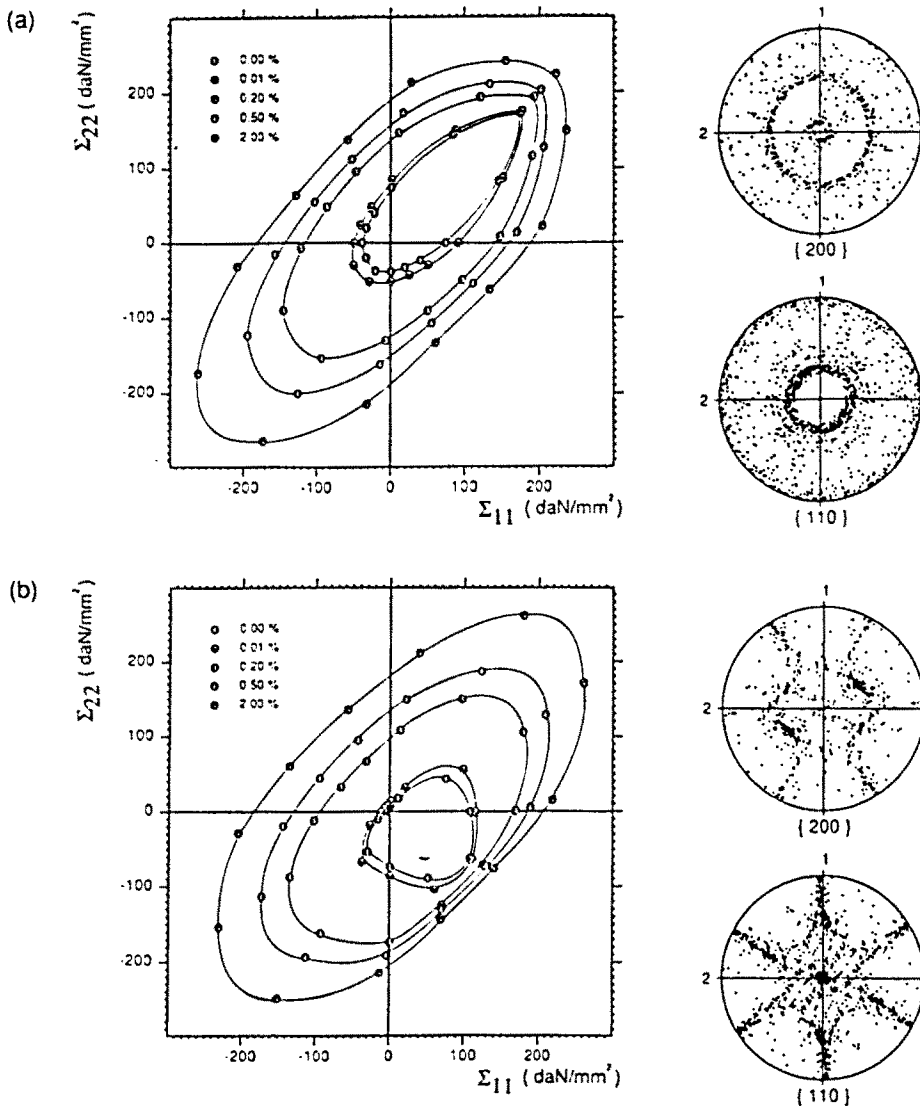


Fig. 4. Subsequent yield surfaces and corresponding crystallographic textures for the different preloading directions. (a) Equibiaxial prestraining up to  $E_{eq} = 0.6$ . (b) Radial loading with  $\Sigma_{11} = -\Sigma_{22}$  until  $E_{eq} = 0.6$ .

At small deformations of FCC and BCC metals two phenomena are in competition, namely multiplication and annihilation of dislocations and their spatial rearrangement. The form of the organization of dislocations varies with the amplitude of plastic strain from irregular clusters toward strongly distinguished cells. For more advanced strains slip bands appear. The dislocations are concentrated inside clusters, cell walls or slip bands which are surrounded by relatively dislocation-free zones. This highly inhomogeneous and incompatible deformation pattern induces third-order residual stresses and associated phenomenon of energy storage which are modelled in the self-consistent approach only in a general sense.

In order to estimate globally the importance of the residual stresses we propose to analyse the evolution of the stored energy  $W_e$  as a function of the plastic strain imposed on the polycrystal.  $W_e$  is the stored energy associated only with the second-order internal stresses. Let  $W_a$  be the anelastic work done during the deformation process whose part  $Q$  is dissipated in the form of heat and another part is stored in the material. Figure 6 shows the evolution of the fraction of stored energy defined as  $F = W_e/W_a$ . The general aspect as well as the magnitude of the calculated quantity is in a good agreement with the experimental observations (Bever *et al.*, 1973).

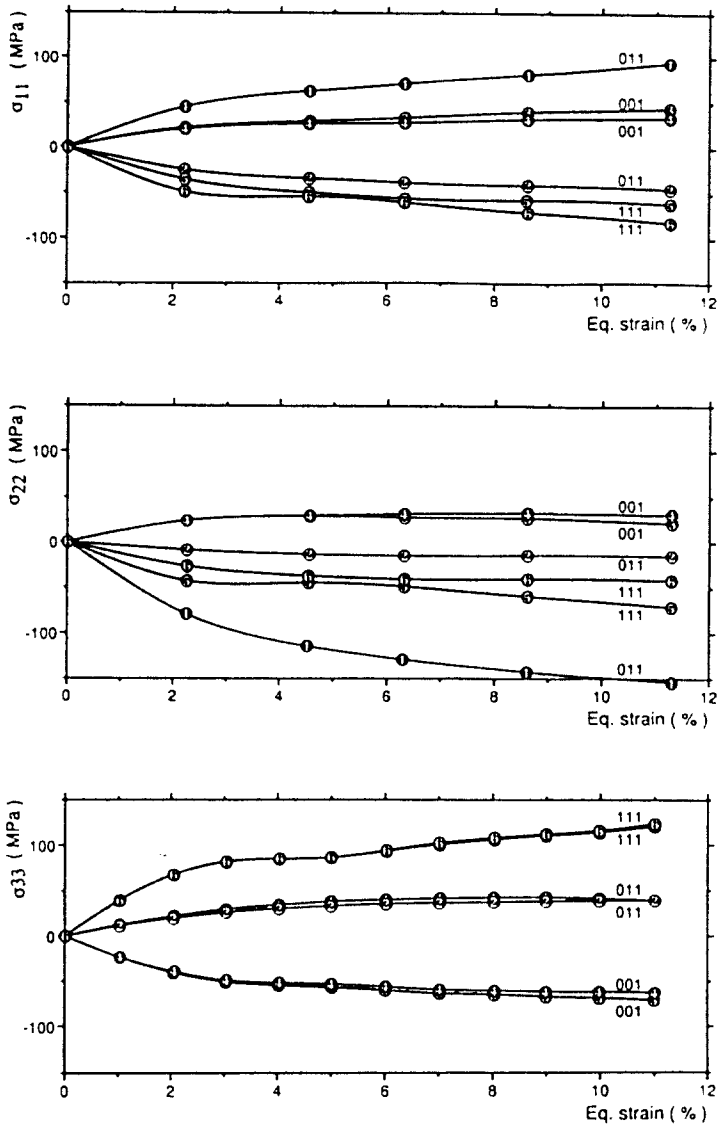


Fig. 5. Residual stress as a function of the equivalent strain during a tensile test in direction 3. The different curves correspond to the orientation of the tensile axis with respect to the lattice.

Figure 7 shows the evolution of the stored energy during a complex loading path. Here the tensile preloading of up to 20% of the plastic strain is followed by the compression test. The mechanical release of the stored energy is observed at the beginning of the compression. This release can be associated with the relaxation of internal stresses due to activation of different slip systems than that active during the tensile deformation which introduced a particular pattern of internal stresses. Analogous evolutions of the stored energy were observed experimentally (Bever *et al.*, 1973). This phenomenon plays an important role in the developmental processes for which the straining paths are not proportional, leading to local plastic instabilities.

Figure 8 presents the evolution of the crystallographic texture during rolling of a BCC metal. Two types of pole figures are drawn, namely the 200 and 110 poles. The initially random texture is shown at the top of the figure, followed by the same poles at 20% and 90% of plastic strain. The comparisons with the experimental measurements by Donadille (1989) are also presented. A very good agreement between the experiment and the self-consistent prediction is visible. This agreement assures the good description of the elasto-plastic anisotropy of the material because the crystallographic texture is the principal factor of this anisotropy.

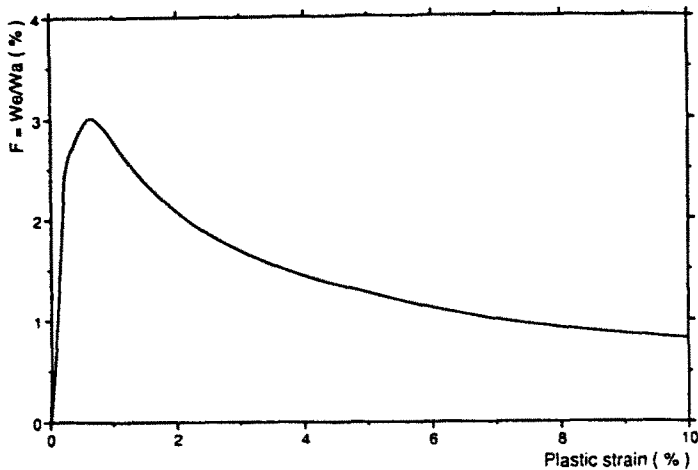


Fig. 6. Evolution of the fraction of stored energy as a function of the plastic strain.

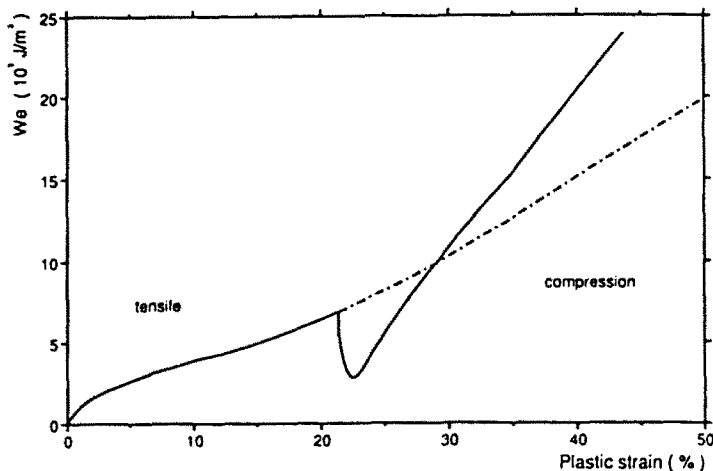


Fig. 7. Mechanical release of the stored energy during a non-proportional tensile-compression loading path.

#### 4. DISCUSSION AND CONCLUSION

The aim of this contribution was to present some global and more local results obtained by the classical self-consistent model applied to the elastoplastic behaviour of polycrystals at large strains. Despite a qualitative and quantitative agreement between the theoretical and the experimental results, such an approach has its limits, which may be divided into two groups.

(i) The first limitation has its origin in the fact that the classical self-consistent approach is only an approximation of the general integral equation solving complex bounding value problems for the microinhomogeneous body. In the frame of this integral equation, other approximations may be developed in order to take into account some specific microstructures. For example, in the case of strongly inhomogeneous two-phase materials, a multisite self-consistent scheme (Fassi-Fehri *et al.*, 1989) or a three-phase composite model (Zaoui *et al.*, 1990) may be used. Nevertheless in the case of usual single-phase polycrystals the limitation at large (or sometimes small) strains of the classical self-consistent model results more from the intragranular-induced microstructure than from the granular characteristics of the polycrystal.

(ii) Due to the assumption of homogeneous plastic strain or strain rate inside the grains, the strain-induced intragranular microstructures are neglected. They correspond to the heterogenization of dislocation density during the plastic flow.

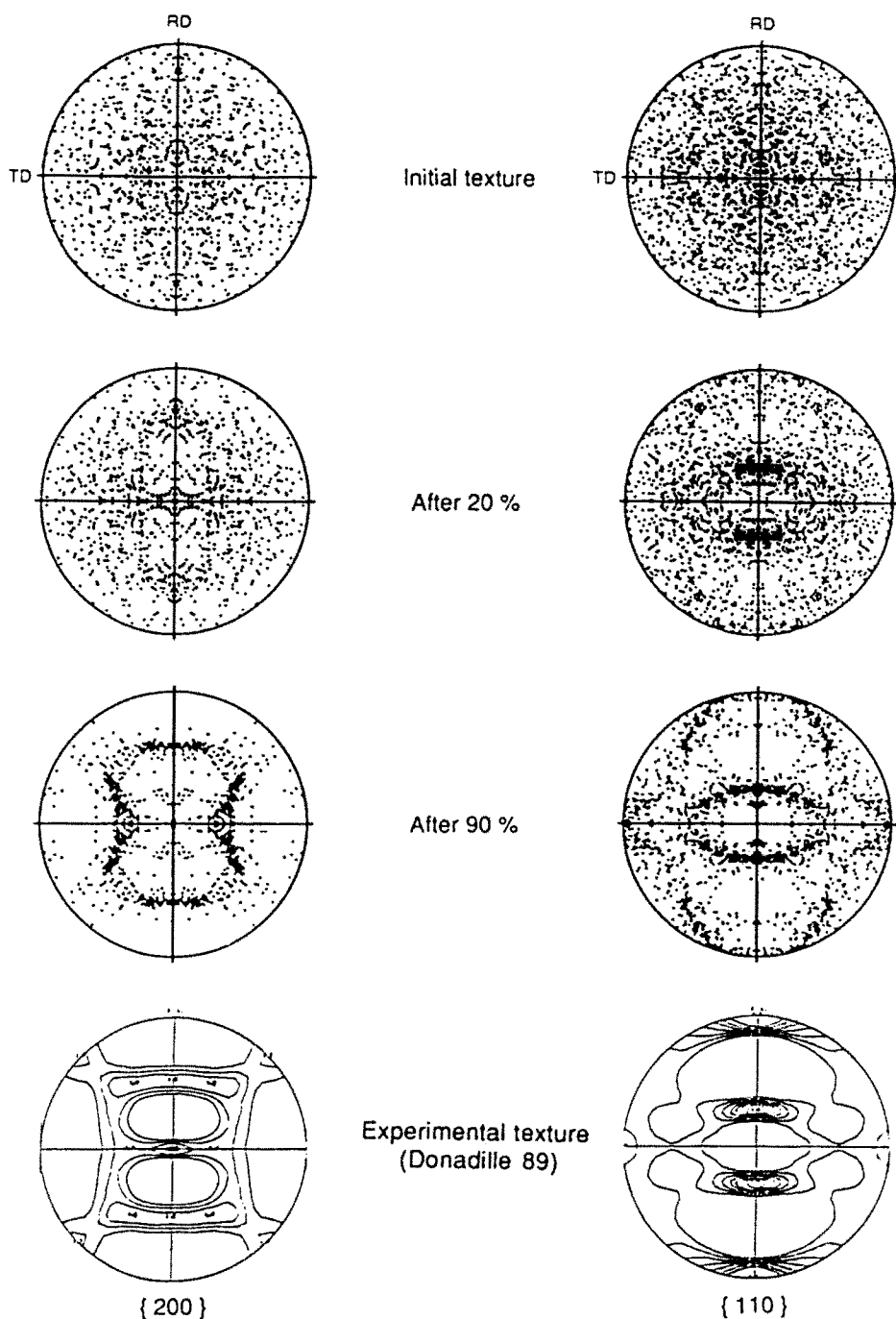


Fig. 8. The evolution of the crystallographic textures for rolling test and comparison with the experimental pole figures obtained by Donadille (IRSID).

From these points of view, interactions between grain boundaries and slip systems are taken into account only in a special manner (surface dislocations).

Effects such as pile-ups are absent in such models so that grain size effects are no longer present in the numerical results when they are experimentally well established. In the same way, the formation of dislocation substructures, i.e. cells and walls poorly described by the hardening matrix, mean that phenomena like microshear-banding and (or) transgranular slip cannot be reproduced by such models. This explains why the obtained results correspond better to high stacking fault energy metals for which the multislip mechanism is the principal deformation mode.



## REFERENCES

- Berveiller, M. and Zaoui, A. (1979). An extension of the self-consistent scheme to plastically-flowing polycrystals. *J. Mech. Phys. Solids* **26**, 325–344.
- Berveiller, M. and Zaoui, A. (1984). Modelling of the plastic behavior of inhomogeneous media. *J. Engng Mater. Technol.* **106**, 295–298.
- Bever, M. B., Holt, D. L. and Titchener, A. L. (1973). Stored energy in cold work. *Prog. Mater. Sci.* **17**, 1–190.
- Budiansky, B. and Wu, T. T. (1962). Theoretical prediction of plastic strains of polycrystals. In *Proc. 4th U.S. National Congress of Applied Mechanics*, ASME, New York, pp. 1175–1185.
- Bunge, H. J. (1969). *Mathematische Methoden der Texturanalyse*. Akademik-Verlag, Berlin.
- Dederichs, P. H. and Zeller, R. (1973). Variational treatment of the elastic constants of disordered materials. *Z. Phys.* **259**, 103–113.
- Donadille, Ch. (1989). Private communication (IRSID).
- Eshelby, J. D. (1957). The determination of the elastic field of an ellipsoidal inclusion, and related problems. *Proc. R. Soc. Lond.* **A241**, 376–396.
- Fassi-Fehri, O., Hihni, A. and Berveiller, M. (1989). Multiple site self consistent scheme. *Int. J. Engng Sci.* **27**, 495–502.
- Franciosi, P. (1983). Glide mechanisms in BCC crystals. *Acta Metall.* **31**, 1331–1341.
- Franciosi, P., Berveiller, M. and Zaoui, A. (1980). Latent hardening in copper and aluminium single crystals. *Acta Metall.* **28**, 273–283.
- Hervé, E. and Zaoui, A. (1990). Modelling the effective behavior of nonlinear matrix-inclusion composites. *Eur. J. Mech. Solids* **9**, 505–515.
- Hill, R. (1965). Continuum micro-mechanics of elastoplastic polycrystals. *J. Mech. Phys. Solids* **13**, 89–101.
- Hutchinson, J. W. (1970). Elastic-plastic behaviour of polycrystalline metals and composites. *Proc. R. Soc. Lond.* **A319**, 247–272.
- Iwakuma, T. and Nemat-Nasser, S. (1984). Finite elastic-plastic deformation of polycrystalline metals. *Proc. R. Soc. Lond.* **A394**, 87–119.
- Jaoul, B. (1964). *Etude de la plasticité et application aux métaux*. Dunod Ed., Paris.
- Kröner, E. (1958). Berechnung der elastischen Konstanten des Vielkristalls aus den Konstanten des Einkristalls. *Z. Phys.* **151**, 504–518.
- Kröner, E. (1967). Elastic moduli of perfectly disordered composite materials. *J. Mech. Phys. Solids* **15**, 319–329.
- Lipinski, P. and Berveiller, M. (1989). Elastoplasticity of microinhomogeneous metals at large strains. *Int. J. Plast.* **5**, 149–172.
- Lipinski, P., Krier, J. and Berveiller, M. (1990). Elastoplasticité des métaux en grandes déformations: comportement global et évolution de la structure interne. *Rev. Phys. Appl.* **25**, 361–388.
- Mura, T. (1982). *Micromechanics of defects in solids*. Martinus Nijhoff, Boston.
- Taylor, G. I. (1938). Plastic strain in metals. *J. Inst. Metals* **61**, 307–324.